Accepted Manuscript

Structural, magnetic and electronic properties of Cu-Fe nanoclusters by density functional theory calculations

C.S. Cutrano, Ch.E. Lekka

PII: S0925-8388(16)33908-1

DOI: 10.1016/j.jallcom.2016.11.425

Reference: JALCOM 39922

To appear in: *Journal of Alloys and Compounds*

Received Date: 31 July 2016

Revised Date: 25 November 2016

Accepted Date: 30 November 2016

Please cite this article as: C.S. Cutrano, C.E. Lekka, Structural, magnetic and electronic properties of Cu-Fe nanoclusters by density functional theory calculations, *Journal of Alloys and Compounds* (2017), doi: 10.1016/j.jallcom.2016.11.425.

$Cu_{12}Fe$ nanocluster's *superior* magnetic moment 3.6 μ_B ↑ on Fe atom due to:

Spin up

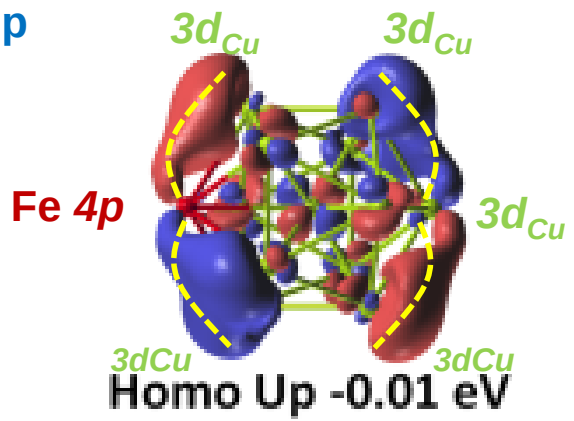

$4p_{Fe}$–$3d_{Cu}$ and $3d_{Cu}$-$3d_{Cu}$ bonding hybridizations

Spin down

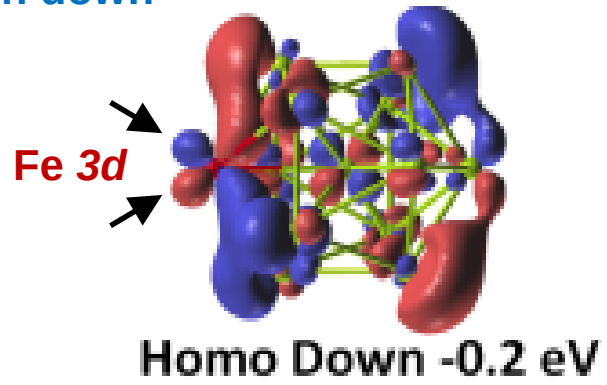

Fe 3d dangling bonds
$3d_{Fe}$–$3d_{Cu}$, $3d_{Cu}$-$3d_{Cu}$ bonding hybridizations

Structural, magnetic and electronic properties of Cu-Fe nanoclusters by density functional theory calculations.

C.S. Cutrano, Ch.E. Lekka*

Department of Materials Science & Engineering, University of Ioannina, Greece

KEYWORDS "Clusters; electronic properties; density functional theory"

ABSTRACT: We present results from density functional theory calculations referring to the magnetic properties of 13, 55, 147 and 309 atoms Cu-Fe icosahedral nanoclusters. Aiming in finding the nanocluster with the optimum magnetic moment (μ_B) we explored the various sizes considering several compositions and atomic conformations. It came out that configurations with agglomerated Fe atoms inside the Cu-Fe nanoclusters and pure Cu surface shell are energetically favoured as demonstrated e.g. for the $Cu_{49}Fe_6$ with $2.3\mu_B$ compared to $2.1\mu_B$ of the Fe bcc. The highest magnetic moment, $3.6\mu_B$, was found in the $Cu_{12}Fe$ case with the Fe atom located at the surface cell, while $3.18\mu_B$ was found for the $Cu_{297}Fe_{12}$ in a similar configuration having Fe atoms surrounded by Cu that occupy the surface shell's edges. The magnetic moment is mainly due to Fe's spin up - down electronic density of states difference close to the Fermi level (E_F). In particular, the Spin-up Fe *d* electronic density of states are fully occupied yielding wavefunctions with homogeneous change distribution while the Spin-down is almost unoccupied exhibiting dangling bonding states close to E_F. These results could be used for the design of environmental sustainable smart alloys with superior magnetic properties e.g. by depositing Fe or FeCu

on Cu nanoclusters or including new elements that provide the possibility of keeping the Fe Spin up-down electronic occupation difference close to E_F.

1. Introduction

Environmentally friendly and sustainable magnetic nanoclusters and coatings are currently under investigations aiming in answering specific technological demands, like superior magnetic properties, thus being promising for several applications such as drug delivery, high-density magnetic recording, catalysis, sensors and for the production of innovative nano-robotic platforms [1 - 6].

Extensive studies revealed that alloying the classical Fe ferromagnet with non-magnetic elements, like Cu, provides the possibility of tailoring the magnetic properties interplaying with the crystallographic structure, especially in systems with reduced dimensions like thin films [7-12]. In particular, experimental studies demonstrated that Fe thin films on Cu(001) having up to 5 monolayers (ML) exhibit fct structure resulting in magnetic moment (MM) up to 2.5μ_B, compared to (2.1-2.15 μ_B) of the Fe bcc [9, 10, 12]. In addition, it came out that above 5 ML of Fe, the fct structure and the ferromagnetic behaviour are altered, while an fct to bcc phase transition occurs for thicker films, above 10 Fe ML [10, 12]. Theoretical studies on Fe/Cu(001) also found that the MM is maximum at the topmost Fe surface layer (2.78-2.85 μ_B), while it gradually decreases for the layers underneath, to reach almost zero MM when the Cu(001) substrate is reached [11, 12]. Focusing on the Fe ML on Cu(111), calculations referring to Fe coverage from 0.25 to 1 ML on Cu(111) yielded that the highest MM is 3.18 μ_B for the 0.25ML, while the lowest is 2.7 μ_B in the case of 1 Fe ML coating [8,9]. It is worth mentioning that in the case of a free standing monoatomic Fe wire, the bridge atom exhibits 3.3 μ_B [13].

Theoretical studies on Fe_{13} and $Fe_{12}Cu$ nanoclusters reported the icosahedral structure as the energetically favoured and that the local MM on the Fe shell varies from 2.8 up to 3.54μ_B [1, 5]. The pure Fe_{55}, Fe_{147} and Fe_{309} yielded for the outermost shell 3.19 μ_B, 3.07 μ_B and 2.98μ_B, respectively, which are much higher than the MM for the core Fe atom (1.90 μ_B, 1.87 μ_B and 1.80 μ_B) [1, 3]. In addition, at E_F the Fe_{13}, Fe_9Cu_4 and Fe_{55} exhibit higher electronic occupation for the spin majority than the spin minority, resulting in a small energy gap, thus classifying these clusters as half-metallic, contrary to the Fe_{147} icosahedral cluster that was found metallic [1, 6]. Ab initio calculations found that Fe nanoclusters composed by less than 100 atoms are more stable in fcc-like structures (icosahedral/cuboctahedral), while larger clusters (up to 561 atoms) prefer bcc-like outermost shell structures although retaining in their cores the smaller clusters' fcc-like structure [4]. In addition, experimental studied reveal that the Fe13 nanocluster most possible has icosahedral structure [14] while the magnetic moments of Fe clusters having from 25 up to 130 atoms was around 3μB /atom and decreases towards the bulk value (2.2μB /atom) for bigger nanoclusters (near 500 atoms) [15]. Nevertheless, the icosahedral structure is always favoured for the clusters of traditional fcc metals like Au, Cu and Ag [16-18] while the experimental production of pure Cu icosahedral nanoclusters with diameter less than 3.8nm has been achieved [19].

It turns out, therefore, that the enhanced MM in systems with reduced dimensions, like Fe nanoclusters and Fe thin films (up to 5ML) on Cu surfaces, contrary to the intuition that no MM enhancement is to be expected from the alloying of a magnetic (Fe) and a nonmagnetic (Cu) element, demonstrates the importance of the crystalline structure, size and interfaces in magnetism. In the present work we performed a systematic study on the Cu-Fe nanoclusters aiming in finding the optimum configuration and cluster's size exhibiting the highest MM. Taking into account that the Fe ML on Cu(111) has the same structure with the icosahedral cluster's faces and could be considered as an infinite cluster's surface, it will be also provided for comparison reasons.

2. Computational details

We used standard Kohn–Sham self-consistent Density Functional Theory (DFT) and to the local density (LDA) and generalised gradient (GGA) approximations by means of the SIESTA code. For all elements the core electrons were replaced by norm-conserving pseudopotentials in the fully nonlocal Kleinman–Bylander [20] form and the basis set was a linear combination of numerical atomic orbitals (NAOs) constructed from the eigenstates of the atomic pseudopotentials [18]. In order to improve the description of the core valence interactions the nonlocal partial core exchange correlation correction was included for Cu [21], while for the Fe case, the pseudopotential was evaluated for the cases of 2dimensioned materials and dimmers [22]. We considered several configurations for the Cu-Fe icosahedral 13, 55, 147 and 309 atoms' clusters along with the pure element clusters aiming in verifying the energetically favoured and the highest magnetic moment configuration. For the geometry optimization, the structure is considered fully relaxed when the magnitude of forces on the atoms were smaller than 0.05 eV/nm.

3. Results and discussion

3.1. Energetics and magnetic moment

Starting with the smallest 13 $Cu_{12}Fe_1$ cluster we considered two cases: a) Fe core atom for which we found the cluster's binding energy (Eb) of -3.35eV and Fe atom's partial MM of 1.93↑μ_B and b) Fe surface atom (1^{rst} shell) with Eb=-3.16eV and Fe MM of 3.60↑ μ_B. (4.00↑ μ_B when using GGA) Interestingly, while the energetically favoured cluster is the one with Fe core atom, the Fe at the surface case yields the highest MM. It should be noted that the pure Fe_{13} exhibits MM of 2.64↑ μ_B for the Fe core atom and 3.40↑ μ_B for each Fe surface atom, while the Cu_{13} exhibits a rather small MM of 0.27↑ μ_B and 0.39↑ μ_B, respectively. The larger MM at the 1rst shell compared to the core are in line with previous calculations on Fe clusters and $Cu_{12}Fe$ [1,3,5]. For the case of the 55 atom Fe-Cu clusters we performed a detailed

study considering several configurations and Fe compositions, Fig.1 aiming to understand the behavior of the magnetic moment. Concerning the $Cu_{54}Fe_1$ cases, we found that the energetically favored refers to the one having the Fe atom in the 1^{rst} shell, while the highest MM (3.26↑ μ_B) when the Fe atom is located at the edge of the 2nd shell (cluster's surface), denoted as Edge position hereafter. For the outermost Cu shell there are two interesting basic cases: 1) Fe atoms full-cover the cluster's resulting in the $Cu_{49}Fe_6$ composition and 2) Fe atoms occupy the Edge sites giving the $Cu_{43}Fe_{12}$ composition. To this end these two main compositions where depicted for further investigation while the full Fe first (Cu43Fe12) and outermost (Cu13Fe42) shell cases along with the Fe_{55} were also considered for comparison reasons. The $Cu_{49}Fe_6$ clusters follow this behavior having the highest MM (3.33↑ μ_B, 3.39↑ μ_B with GGA) when Fe atoms occupy Edge sites, while the energetically favoured configuration corresponds to the agglomerated Fe atoms in the 1_{rst} shell (-4.08eV). The $Cu_{49}Fe_6$ agglomerated Fe atoms' case on the 2nd shell suggests that the Fe atoms occupy the triangle side (Side positions hereafter) of the surface and are energetically more stable (-4.01eV) than the corresponding Edge case (-3.97eV) and has lower MM (3.06↑ μ_B). Nevertheless, the Edge and the Side cases correspond to the 'boundary' cases in the sense that any other configuration with Fe surface atoms will have energy and MM values within these limits. Similar results stand for the $Cu_{43}Fe_{12}$ clusters, while the Fe_{55} cluster yields 3.26↑ μ_B in the 2nd shell. These results reveal the importance of the location of the Fe atoms, i.e. in order to increase their MM they have to be located at the cluster's Edge positions and surrounded only by Cu first neighbours. For this reason, we will focus on the surface Edge and Side (agglomerated) cases of $Cu_{49}Fe_6$ that also stand for the Fe composition of 10at%.

For the 147 and 309 Cu-Fe clusters we also focused on the surface Edge and Side Fe atom cases keeping the Fe composition less than 10at%. For the $Cu_{135}Fe_{12}$ Edge cluster we found -4.34eV and 3.25↑ μ_B (3.26↑ μ_B with GGA), while for the $Cu_{138}Fe_9$ Side cluster -1.53 eV and 2.73↑ μ_B (2.90↑ μ_B with GGA),., thus being unfavoured. Similar behavior we found for the $Cu_{297}Fe_{12}$ Edge cluster with energy of -4.74eV

and MM of 3.18↑ μ_B, (3.22↑ μ_B with GGA), while the $Cu_{294}Fe_{15}$ Side cluster has -4.73eV and 2.74↑ μ_B (2.96↑ μ_B with GGA). These results also consolidate the finding that in order to increase the MM the Fe atoms need to be located at Edge positions and to have Cu first neighbours.

3.2. **Electronic and magnetic properties**

In Fig.2 we present the spin polarized total and partial electronic density of states (EDOS) for a) 13 and b) 55 clusters when Fe atoms occupy the *Edges* sites as in the first's column insets. In addition, in the second's column insets the 147 and 309 Edge and Side EDOSs are presented for comparison reasons. In Fig2c the EDOS of Fe ML on Cu(111) is also shown. The EDOS of the smallest 13 atom cluster exhibits discrete and localized states, while as the size of the cluster increases the peaks become wider approaching the band characteristics of the Cu(111). The Cu and Fe 3d states are situated between -6 eV and -2eV, while the 4s electrons and Cu 3p semi-core mainly exist in the low energy states and close to E_F. From the partial EDOS we can clearly see that the Fe PEDOS is mainly responsible for the spin up-down differences, especially close to the E_F, thus inducing the magnetic moment. In addition to magnetism, the $Cu_{12}Fe$ cluster is half-metallic due to the electronic contributions at E_F only in the spin majority EDOS, in line with a previous theoretical study on Fe_{13} and Fe_9Cu_4 [6]. In particular, the spin up EDOS in occupied at E_F mainly due to Cu 3d and Fe 4p electrons (that are partially filled, $0.3e^-$, upon cluster's formation), while the Fe 4s contribute in the states around -0.2eV. On the contrary, the $Cu_{12}Fe$ spin minority EDOS has an energy gap of 0.4eV between the highest occupied and the lowest unoccupied molecular orbital (named HOMO and LUMO respectively) mainly due to Fe 3d and Cu 3d electrons.

The 55 atom $Cu_{49}Fe_6$ clusters' spin up EDOS exhibits E_{gap} of 0.7eV for the Edge case, while in the spin down EDOS the corresponding Egap is almost zero (0.08eV), thus yielding, half-metallic character, in line with previous ab initio calculations on the Fe_{55} [3]. The spin up EDOS at the E_F is mainly due to

Cu and Fe 3d occupation, while in the corresponding spin down EDOS the Fe 3d electrons are dominant. The 13 and 55 CuFe clusters' half-metallic character is altered as the size of the cluster increases. In the inset of Fig2b's second column, the total EDOS of the 147 atoms $Cu_{135}Fe_{12}$ (Edge) and $Cu_{137}Fe_{10}$ (Side) clusters are presented where small differences between the two cases and spin up-down deviations are depicted mainly close to E_F. The absence of an energy gap reveals the metallic features of the alloys 147 atom clusters, similarly to the pure Fe_{147} cluster [3]. Similarly, the 309 $Cu_{297}Fe_{12}$ (Edge) and $Cu_{294}Fe_{15}$ (Side) clusters exhibit metallic character, in agreement with the alloys and pure 147 clusters and the pure Fe_{309} [3], while visible differences between the two configurations are only depicted close to E_F. Finally, Fig 2c depicts the EDOS of the Fe ML on Cu(111) that manifests metallic character mainly due to both atoms' 3d occupation. In addition, the Fe 3d electrons are responsible for the spin up-down EDOS differences and the resulting magnetic moment.

Aiming in understanding the electronic hybridizations that result in the different spin up and spin down EDOS occupations we plotted the wavefunctions (WF) close to E_F focusing on the HOMO states. In Fig.3a depicts the $Cu_{12}Fe$ cluster's structure, MM and selective WFs. It comes out that the Fe atom has the highest MM (3.6↑ μ_B) from all the understudy cases, Fig.2a, due to the almost fully occupied Fe 3d EDOS and to the partial filling of the Fe 4p electrons (0.3e^-) due to charge transfer from Fe 3d and Cu atoms. Indeed, in the HOMO spin up at E_F (-0.01 eV), the Fe' 4p lobes reveal Fe 4p – Cu $3d_{t2g}$ hybridization, shown as red or blue lobes, mainly with the neighbouring Cu atoms (1 or 2 labelled atoms), respectively, Fig.3a. In addition, Fe's symmetrical Cu atom (named 3) reveals Cu $3d_{t2g}$ – Cu $3d_{t2g}$ hybridizations with its 4 - 5 Cu neighbouring atoms. On the contrary, the HOMO spin down situated at -0.2eV at the Egap's energy boundary reveals two free dangling lobes on the Fe $3d_{t2g}$ orbital and two hybrid lobes with the Cu (1 and 2) neighbouring atoms. The symmetrical 3 Cu atom retains the HOMO spin up behaviour. The spin up WF at -0.2eV also shows dangling bonds on both Fe and the Cu (3) 4s orbitals and therefore anti bonding features with the neighbouring atoms. Concluding in the $Cu_{12}Fe$

cluster the filling of the Fe 4p electrons in the HOMO up is the reason of the metallic features, while the different electron occupation between the spin up and down WFs is the origin of the magnetic moment.

The $Cu_{49}Fe_6$ HOMO spin up WF (-0.1eV) has equivalent $3d_{t2g}$ electron distributions in all Fe and Cu atoms, while the spin down HOMO WF (-0.03eV) is mainly attributed to the Fe $3d_{eg}$ orbital exhibiting dangling lobes on the Fe $3d_{t2g}$ orbital, in line with the corresponding $Cu_{12}Fe$ spin down HOMO WF. This Fe $3d_{eg}$ spin down state plays critical role in the presence of magnetic moment since it establishes one of the major differences between spin up-down Fe PEDOS in Fig. 2b.

In the $Cu_{135}Fe_{12}$ cluster the HOMO up shows mirror symmetry mainly due to Fe_1 and Fe_2 4s electrons, while the nearby energy states exhibit the same WFs' features, although in different Fe-Fe axes. The $Cu_{135}Fe_{12}$ HOMO spin down WF is similar to the corresponding $Cu_{49}Fe_6$'s HOMO spin down revealing Fe $3d_{eg}$ and Cu $3d_{t2g}$ occupations and dangling bonds on the Fe orbitals. For both cases the highest electron occupation is depicted in the outermost cell where the Fe atoms are located revealing their role in the presence of magnetic moment. Finally, the biggest $Cu_{297}Fe_{12}$ cluster exhibits Cu-Cu hybridizations and enhanced electron contribution in the two outermost cells, while the HOMO spin down WF is mainly localized on the Fe $3d_{t2g}$ orbitals and in the cluster's centre yielding the differences between the spin up and down WFs.

Concluding, the filling of the Fe 4p orbital in the $Cu_{12}Fe$ cluster, the Fe 4s contribution close to Fermi level for the $Cu_{135}Fe_{12}$ and the homogeneous change distribution of the Fe 3d and Cu 3d electrons in the $Cu_{49}Fe_6$ and $Cu_{297}Fe_{12}$ are responsible for the almost fully electron occupations in the spin up EDOS. On the contrary, the Spin-down EDOSs are almost unoccupied exhibiting dangling bonding wavefunctions close to E_F. These spin up- spin down EDOS and wavefunctions differences are the electronic origin of the MM.

Fig.4 depicts the clusters' size dependence of MM per Fe atom for the GGA and LDA cases of the Cu-Fe Edge and Cu-Fe Side clusters as well as the Fe monolayer on Cu (001) and Cu(111) surfaces and

available theoretical and experimental results for comparison reasons. We observe that the LDA and GGA provide a bottom and upper limit of the magnetic moment. We clearly see that the highest MM corresponds to the $Cu_{12}Fe$ cluster (independently whether it refers to edge or side Fe locations), while as the clusters' size increases the MM drops. The CuFe Edge clusters have bigger MM, saturating around $3.2\mu_B$, than the corresponding Side cases, saturating at $2.7\mu_B$ ($2.96\mu_B$ with GGA) and pure Fe $2.9\mu_B$ clusters using GGA [3]. In addition, these theoretical results are in line with the experimental data on the magnetic moments of Fe clusters which found that from 25 up to 130 atoms the MM is around 3μB /atom and decreases towards the bulk value (2.2μB /atom) for bigger nanoclusters (close to 500 atoms) [15]. It is interesting to mention that although the calculations refer to clusters, the outcome can be extended to films and bulk systems. Indeed, we note that as the triangle side of the icosahedral clusters increases we see that the CuFe cluster's MM converge to the Fe ML on Cu(111). In addition, the $CuFe_{12}$, exhibits slightly smaller MM ($3.5\mu_B$), compared to $Cu_{12}Fe$ and Fe_{13} [1,3,5]. In the same figure we also provide the available [8] and present ab-initio Fe ML on Cu(111), as well as the Fe fcc [3] and Fe bcc cases [1] while the results of the Fe ML on Cu(001) shows higher MM than the corresponding (111) surface. Finally, an oxygen atom was placed next to an Fe edge atom as a first step towards the investigation of the oxidation process (orange line). We found that although that the MM of that Fe atoms decreases (e.g. from $2,98\mu_B$ to $3.39\mu_B$ with GGA) it still remains higher than the surface and the bulk cases while the other edge Fe atoms almost retain their initial values ($3.37\mu_B$ with GGA). It turns out that in all cases the nano-clusters exhibit larger MM than the Fe thin films and bulk systems.

4. **Conclusions**

We studied the structural, electronic and magnetic properties of the Cu-Fex (x<10%). We found that configurations with agglomerated Fe atoms inside the Cu-Fe nanoclusters and pure Cu surface shell are

the energetically favoured while the highest MM per Fe atom was found when the Fe atoms are located at the Edge sites of the surface shell having Cu first neighbours.

The CuFe MM is related to the spin up - down EDOSs differences that are mainly situated close to the Fermi level. In particular, the Spin-up Fe *d* electronic density of states are fully occupied yielding wave-functions with homogeneous change distribution while the Spin-down is almost unoccupied exhibiting dangling bonding states close to E_F. The 13 and 55 clusters are almost half-metallic, while the 147 and 309 cluster exhbit mainly metallic features, in line with the Fe clusters [4]. In all cases the nano-clusters exhibit larger MM than the Fe thin films and bulk systems while the alloy Side cluster's MM was found to decrease towards the Fe ML on Cu(111) value, to reach a plateau above 120 atoms.

These results could be of use for the design of CuFe clusters and cluster-coating with improved magnetic properties.

Acknowledgement

This work was supported by the SELECTA (No. 642642) H2020-MSCA-ITN-2014 project.

References

(1) R. Singh, P. Kroll, Structural, electronic, and magnetic properties of 13-, 55-, and 147-atom clusters of Fe, Co, and Ni: A spin-polarized density functional study, Phys. Rev. B 78 (2008) 245404

(2) N J O Silva, J S Amaral, V S Amaral, B F O Costa, G Le Caer, Superferromagnetism in mechanically alloyed fcc Fe23Cu77 with bimodal cluster size distribution, J. Phys.: Condens. Matter 21 (2009) 046003

(3) Cheng Zhi-Da, Ling Tao, Zhy Jing, First-principles calculation of magnetism of icosahedral Fe clusters, Chin. Phys. B 19 (2010) 057101

(4) G. Rollmann, M. E. Gruner, A. Hucht, R. Meyer, P. Entel, M. L. Tiago, J. R. Chelikowsky, Shellwise Mackay Transformation in Iron Nanoclusters, Phys. Rev. B 99 (2007) 083402

(5) G.L. Gutsev, L.E. Johnson, K.G. Belay, C.A. Weatherford, L.G. Gutsev, B.R. Ramachandran, Structure and magnetic properties of Fe12X clusters, Chemical Physics 430 (2014) 62-68

(6) A. G. Tefera, M. D. Mochena, Doping icosahedral Fe13 with 3d transition elements, arXiv:1311.7108

(7) P.Ohresser, J. Shen, J. Barthel, M. Zheng, Ch.V. Mohan, M.Klaua, J. Kirschner, Growth, structure and magnetism of fcc Fe ultrathin films on Cu(111) by pulsed laser deposition, Phys. Rev.B 59 (1999) 3696-3706

(8) H. Choi, S.G.Lee, Y.C. Chung, The role of structural vari-ations in the magnetism of Fe/Cu(111): First-principles calculations, Comp.Mater.Scie. 49 (2010) S291-S296

(9) T. Kish, H. Nakamoshi, H. Kasai, A. OKIJ, Magnetic Proper-ties of Fe Thin Films on Cu(111), J. Phys. Soc. Japan 71, (2002) 2983–2985

(10) Th. Detzel, M. Vonbank, M. Donath, V. Dose, Magnetism and structure of ultrathin Fe/Cu001) from spin-polarized appearance-potential spectroscopy, Journal of Magnetism and Magnetic Materials 147 (1995) Ll-L6

(11) X. Yin, K. Hermann, Structural and magnetic properties of ultrathin fcc Fe films on Cu(001): Full potential LAPW studies, Phys. Rev. B 63 (2001) 115417

(12) M. Donath, Magnetic order and electronic structure in thin films, J. Phys.: Condens. Matter 11 (1999) 9421–9436

(13) H. Nakanishi, H. Kasai and A. Okiji, Atom bridge made from magnetic materials: atomic configuration and magnetic properties, Surf. Sci. 493 (2001) 757

(14) M. Sakurai, K. Watanabe, K. Sumiyama, K. Suzuki, Magic Numbers in Fe Clusters Produced by Laser Vaporization Source, Journal of the Physical Society of Japan 67 (1998) 2571-2573

(15) I.M. L. Billas, J. A. Becker, A. Chatelain, W. A. de Heer, Magnetic Moments of Iron Clusters with 25 to 700 Atoms and Their Dependence on Temperature, Phys. Rev. Let. 71(1993) 4067-4070

(16) J. Uppenbrink, D. J. Wales, Structure and energetics of model metal clusters, J. Chem.Phys.96, 11 (1992) 8520-8534

(17) Ch.E. Lekka, G.A. Evangelakis, Bonding characteristics and strengthening of CuZr fundamental clusters upon small Al additions from density functional theory calculations, Scripta Materialia 61 (2009) 974–977

(18) Ch.E. Lekka, Cu–Zr and Cu–Zr–Al clusters: Bonding characteristics and mechanical properties, Journal of Alloys and Compounds 504S (2010) S190–S193

(19) D. Reinhard, B. D. Hall, P. Berthoud, S. Valkealahti, R. Monot, Unsupported nanometer-sized copper clusters studied by electron diffraction and molecular dynamics, Phys. Rev. B, 58 (1998) 4917-4926.

(20) L. Kleinman, D.M. Bylander, Efficacious form for model pseudopotentials, Phys. Rev. Lett. 48 (1982) 1425.

(21) J.Junquera,O.Paz,D.Sanchez-Potal, E.Artacho, Numerical atomic orbitals for linear-scaling calculations Phys.Rev.B 64 (2001) 235111

(22) P. Riveroa, V. Manuel García-Suárezb, D. Pereñigueza, K. Utta, Y. Yanga, Laurent Bellaichea, Kyungwha Parkc, Jaime Ferrerb, Salvador Barraza-Lopez, *Systematic pseudopotentials from reference eigenvalue sets for DFT calculations*, Computational Materials Science **2015**, 98, 372–389

Figure 1

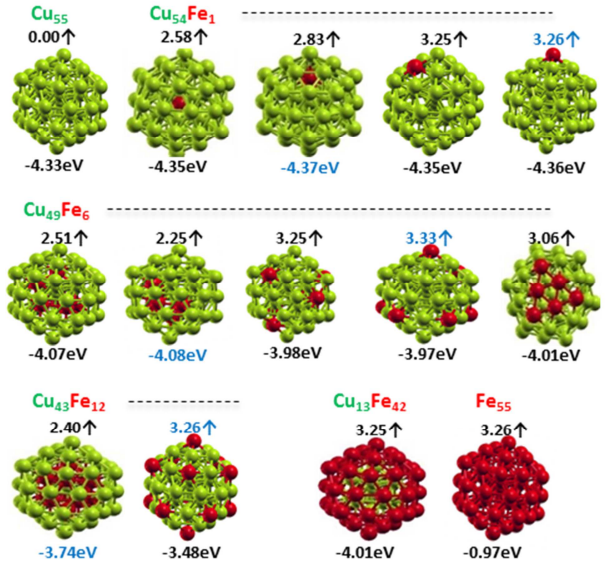

Fig.1. CuFe icosahedral 55 atom clusters along with the corresponding magnetic moment and the binding energy. Green and red spheres stand for the Cu and Fe atoms.

Figure 2

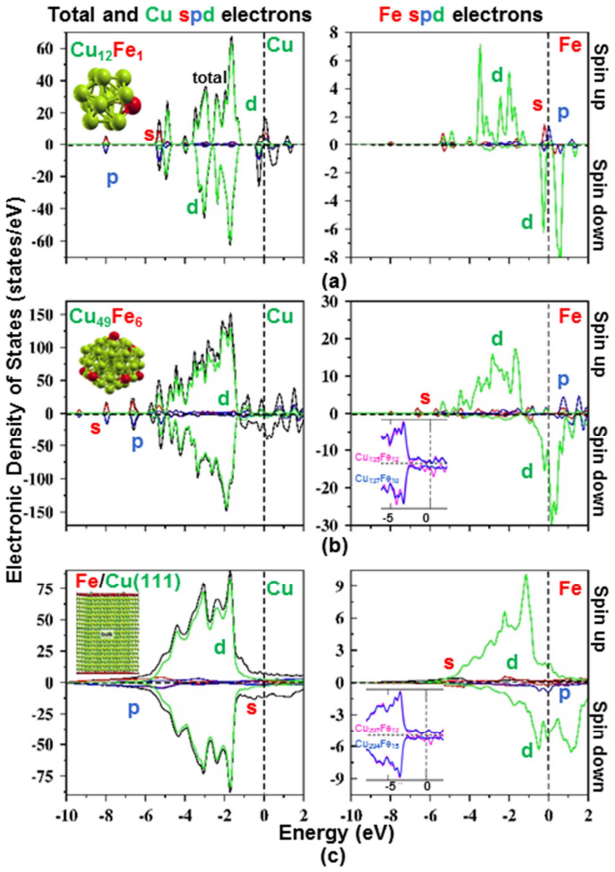

Fig.2 Electronic density of states: a) Cu12Fe, b) C49Fe6 and c) Fe ML on Cu(111). In the (b), (c) insets the total EDOS of Edge and Side cases for 147 and 309 clusters are presented. Black, red, blue and green lines stand for the total, s, p and d electrons' contributions, respectively.

Figure 3

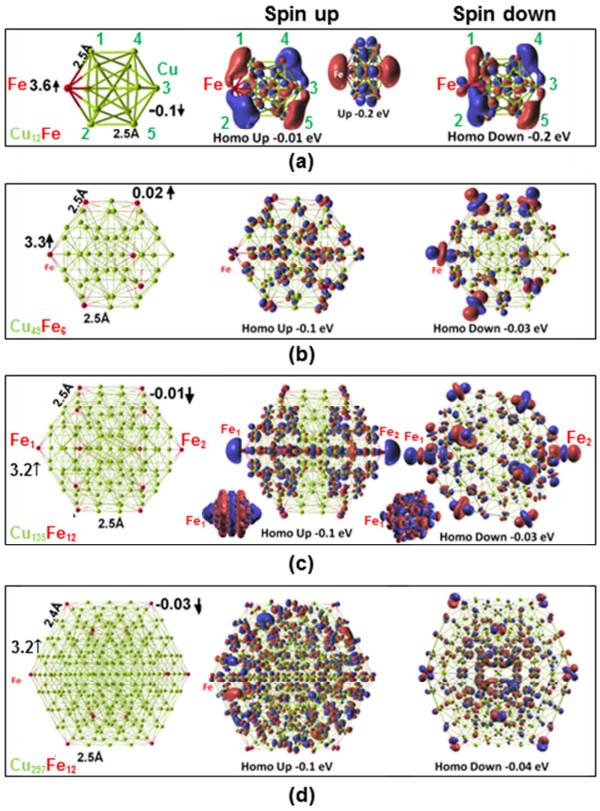

Fig.3. CuFe Edge clusters structure, MM (↑) and HOMO WFs: a) Cu12Fe, b) Cu49Fe, c) Cu135Fe12 and d) Cu297Fe12. The WF's isovalue is set from −0.05 (red) up to +0.05 (blue) e/Å^3.

Figure 4

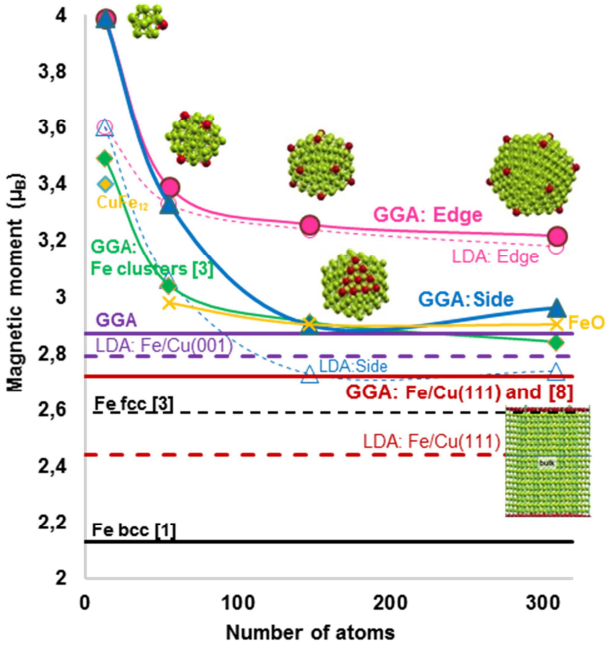

Fig.4. Magnetic moment per Fe atom (μ_B) of the CuFe Edge clusters (GGA/LDA with solid/dashed magenta line/circles), CuFe Side clusters (GGA/LDA with solid/dashed blue line/triangles), Fe clusters (green rhombus, data from [3]), $CuFe_{12}$ (yellow rhombus, data from [3]), Fe ML on Cu(111) (GGA/LDA with solid/dashed red line stand for the results of present work and [8]), Fe ML on Cu(001) (GGA/LDA with solid/dashed purple line), FeO at an edge side (orange line), (Fe fcc (black dashed line, data from [3]) and Fe bcc (black solid line, data from [1]).

Highlights:

- Fe aggregate inside the CuFe nanocluster. The Cu surface shell is energetically favored.
- The 13 and 55 clusters are half-metallic while the 147 and 309 clusters are metallic.
- Fe atoms are mainly responsible for the spin up-down differences close to fermi level.
- Fe dangling bonds in all HOMO spin down states reveals the origin of magnetism .